Limnol. Oceanogr., 48(5), 2003, 1903–1912

Performance of sinking and nonsinking phytoplankton taxa in a gradient of mixing depths

Robert Ptacnik,[1] *Sebastian Diehl, and Stella Berger*
Zoologisches Institut, Ludwig-Maximilians-Universität, Karlstraße 25, 80333 München, Germany

Abstract

According to a recent dynamical model, the depth of a well-mixed water column should have contrasting effects on the abundances of sinking and nonsinking phytoplankton taxa. Because of increasing light limitation, nonsinking taxa should decline monotonically with increasing mixing depth, and because of sinking loss limitation at low mixing depths, sinking taxa should peak at intermediate mixing depths. Along a gradient of mixing depths, the position of this maximum should increase with increasing taxon-specific sinking velocity and decrease with increasing background turbidity. In two field-enclosure experiments, we investigated the effects of mixing depth and background turbidity on a variety of sinking and nonsinking phytoplankton taxa. We exposed the natural, 100-μm-screened phytoplankton community of a clear, unproductive, but silica-rich lake to a gradient of mixing depths (1.5–15 m) during 4–6 weeks. To mimic two different background turbidities, the transparent enclosure walls were surrounded by either white or black foliage. Although diatoms suffered from high sedimentation losses at low mixing depths, they dominated biomass at all mixing depths throughout both experiments. Results were largely in accordance with model predictions. Specific gross growth rates of most common taxa were negatively related to mixing depth. In both experiments, the abundances of most sinking taxa showed a unimodal pattern along the mixing depth gradient, while two of three motile taxa declined monotonically with mixing depth. The depths where these taxa reached their maximal abundances were positively related to taxon-specific sinking velocity and negatively related to background turbidity.

The vertical extension of the mixed surface layer of pelagic aquatic systems (also called mixing depth) is an important parameter in the environment of phytoplankton. Most phytoplankton is passively moved within the mixed surface layer. Its average vertical position therefore decreases with increasing mixing depth. Because light decreases exponentially in the water column, the average availability of photosynthetically active radiation also decreases with increasing mixing depth. As a consequence, primary production (per unit volume) and the concentration of phytoplankton biomass are expected to decrease with increasing mixing depth (Riley 1942; Sverdrup 1953; Huisman and Weissing 1995). Such a pattern has been found in controlled laboratory experiments and in comparative lake data (Petersen et al. 1997; Huisman 1999; Soto 2002). Sverdrup (1953) suggested that, beyond a specific mixing depth (which he called critical depth), the average light intensity is insufficient to support a phytoplankton population. This concept has been successfully applied to oceanic systems with deep and intensively mixed surface layers (Sverdrup 1953; Smetacek and Passow 1990).

Recently, the generality of the expectation of a monotonic decline in phytoplankton density with mixing depth has been questioned. Sedimentation losses of phytoplankton seem to be an important factor that may limit phytoplankton biomass at low mixing depths (Condie and Bormans 1997; Lucas et al. 1998; Diehl 2002; Diehl et al. 2002). Because most phytoplankton taxa have a higher specific mass than water, all nonmotile and negatively buoyant taxa tend to sink out of the epilimnion with time. The specific sedimentation loss rate of a given taxon depends strongly on its sinking velocity. Sinking velocities vary among different species between 0 and 2 m d^{-1}, depending mainly on cell (or colony) size and shape and on specific density (e.g., Smayda and Boleyn 1965; Reynolds 1984, 1988). For example, many diatoms have relatively high sinking velocities because of their silica frustules (Reynolds 1984; Sommer 1994), whereas some cyanobacteria may regulate their density, depending on environmental conditions (Reynolds 1988; Walsby et al. 1989). While sinking velocity is an important determinant of sedimentation losses, the actual sedimentation loss rate depends also on mixing depth. Specific sedimentation loss rates are higher in shallow mixed layers than in deep ones because the probability of an algal cell settling out of a mixed water column decreases with increasing mixing depth (Reynolds 1984; Visser et al. 1996; Diehl et al. 2002).

By affecting light availability and sedimentation losses, mixing depth is a key factor in the environment of phytoplankton (Reynolds 1984; Sommer et al. 1986; Diehl 2002). It should not only affect overall phytoplankton biomass but also its taxonomic composition. In particular, with respect to sedimentation losses, different taxa are influenced by mixing depth in different ways. For example, diatom blooms depend on deep and intense vertical mixing, whereas flagellates are favored by shallow mixed layers or complete stratification (Reynolds et al. 1983, 1984; Huisman et al. 2002). In a lake

[1] To whom correspondence should be addressed. Present address: Institute for Marine Research, Düsternbrooker Weg 20, 24105 Kiel, Germany (rptacnik@ifm.uni-kiel.de).

Acknowledgments

We thank Angelika Wild, Willibald Brosch, Thomas Kunz, and the students of the 1997 and 1998 Aquatic Ecology classes for their skillful help and/or advice during field and laboratory work. We are grateful to Jef Huisman and an anonymous referee for their helpful comments and to Ulrich Sommer for valuable comments on the manuscript. The research was financially supported by a start-up grant from the University of Munich.

where the filamentous diatom *Melosira italica* usually vanishes during summer stratification due to high sedimentation losses, Lund (1971) achieved its persistence in this period by artificial mixing. Similarly, artificial mixing of the water column was the main factor promoting the persistence of diatoms in the phytoplankton community of large lake enclosures (Reynolds et al. 1983, 1984). When mixing depth fell under 2 m, diatoms were excluded from the systems by high sedimentation losses. By artificial mixing of a stratified lake, Visser et al. (1996) initiated a community shift from dominance by buoyant cyanobacteria to dominance by negatively buoyant green algae. A reduction in the sedimentation losses of the green algae was the driving force behind this shift in the phytoplankton community.

Attempts to include the effects of mixing depth on production and sedimentation into conceptual models of phytoplankton dynamics have been rare until recently (Lucas et al. 1998; Huisman et al. 1999, 2002; Diehl 2002; Elliott et al. 2002). In the model by Diehl (2002), phytoplankton production is related to mixing depth and background turbidity (=light attenuation by water molecules and dissolved and suspended substances). The model describes the dynamics of phytoplankton in a well-mixed water column. Light availability, specific production rate, and specific sedimentation rate are all assumed to decrease with increasing mixing depth. Phytoplankton growth is assumed to be co-limited by light and a mineral nutrient and sinking out of the mixed layer is the only loss process included in the model. Assuming that a single taxon dominates phytoplankton biomass, the following, general steady-state predictions for the (volumetric) density of that taxon can be derived from the model (Fig. 1; for derivations, see Diehl 2002): (1) The density of nonsinking phytoplankton should decrease monotonically with increasing mixing depth because light-dependent production decreases with increasing mixing depth (Fig. 1a, species 'zero'). (2) Sinking phytoplankton suffers from high sedimentation losses at very low mixing depths that cannot be compensated for by increased light availability (sedimentation loss rate rises to infinity when mixing depth approaches zero). The density of sinking phytoplankton should therefore show a unimodal trend along a gradient of mixing depths (Fig. 1a; species 'low' and 'high'). (3) Everything else being equal, phytoplankton density should decrease with increasing sinking velocity. Additionally, the mixing depth at which phytoplankton reaches its maximum density should increase with increasing sinking velocity (Fig. 1a). (4) Phytoplankton density decreases with increasing background turbidity. For sinking phytoplankton taxa, the peak in the abundance versus mixing depth relationship should occur at a shallower mixing depth when background turbidity is increased (Fig. 1b).

Although, strictly speaking, these qualitative predictions apply only to systems with a single phytoplankton species at steady state, we expect them to be robust against deviations from these assumptions. For example, Diehl et al. (2002) investigated the effects of mixing depth and background turbidity on natural, mixed phytoplankton communities in a series of field-enclosure experiments that covered a 10-fold range of mixing depths (1.5–15 m). The responses of total phytoplankton biomass (expressed as algal biovolume) to experimental manipulations corresponded qualitatively very well to the model expectations for a single, sinking taxon (Diehl et al. 2002). Here we report on the taxon-specific responses of the most abundant phytoplankton taxa to the experimental treatments and relate them to the assumptions and the four predictions listed above. This allows us to investigate the effects of mixing depth and background turbidity on species differing in their sinking velocities and their demands on light.

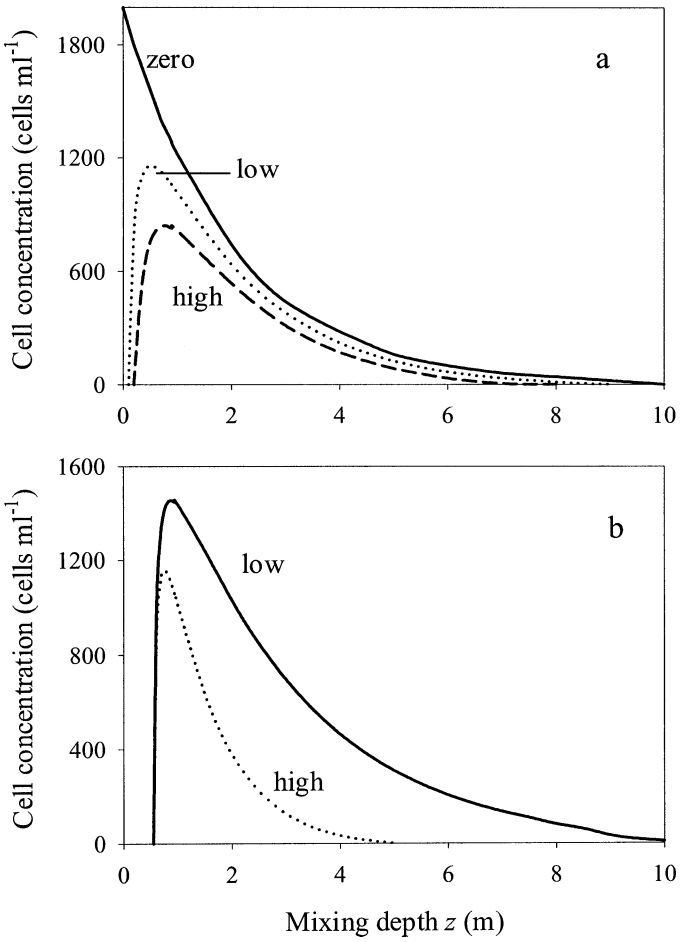

Fig. 1. Effects of (a) sinking velocity and (b) background turbidity on phytoplankton equilibrium density along a mixing depth gradient, as predicted by the closed-system model (Eq. 1) in Diehl (2002). Panel (a) shows otherwise identical species differing only in sinking velocity (zero, low, and high). (b) shows a sinking species under low and high background turbidity. The qualitative differences among the curves described in the text are general and do not depend on the specific choice of parameters (Diehl 2002).

Materials and methods

Study site and sampling—In the falls of 1997 and 1998, we conducted two enclosure experiments in lake Brunnsee, which is situated close to the Limnological Research Station of the University of Munich at Seeon, 90 km east of Munich, southern Germany. Lake Brunnsee is a small, deep, and clear hardwater lake (area 5 ha, maximum depth 19 m, Secchi

depth in summer 7–15 m, alkalinity >4 meq L^{-1}) that is characterized by low concentrations of total phosphorus (7–10 μg L^{-1}) in combination with high concentrations of dissolved inorganic silica and nitrogen (both >3 mg L^{-1}). Throughout most of the summer, concentrations of soluble reactive phosphorus (SRP) are near or below detection limits. Phytoplankton biomass in lake Brunnsee is dominated by diatoms throughout the growing season, with small chlorophytes and filamentous cyanobacteria occurring in low densities (Holzmann 1994).

In both experiments, we exposed the natural phytoplankton community to a gradient of mixing depths in a series of 10 cylindrical plastic bags (diameter 95 cm). These enclosures were suspended from a raft in the middle of lake Brunnsee. In both years, we twice replicated five different enclosure depths (2, 4, 7, 10, and 14 m in 1997; 1.5, 3, 6, 10, and 15 m in 1998). The enclosures were open to the atmosphere and closed at the bottom. Around an inner transparent plastic foliage, the enclosures were covered by a snugly fit layer of opaque white (1997) or black (1998) plastic to simulate different background turbidities. The attenuation coefficient in the 5-m-deep mixed surface layer of the lake was 0.43 m^{-1} in 1997 and 0.36 m^{-1} in 1998. In a water column of 5-m depth, enclosure walls caused an increase in background attenuation by 0.34 m^{-1} (moderate background turbidity, 1997) and 0.96 m^{-1} (high background turbidity, 1998), respectively. To induce constant mixing, air was pumped to the bottom of each enclosure through a small plastic tube for 1 min every 5 min. The mixing was highly effective and we never observed a vertical temperature gradient in any of the enclosures. The experiments started in mid-September and lasted for 27 d (1997) and 42 d (1998), respectively. At the beginning of each experiment, the enclosures were filled with water from the epilimnion of lake Brunnsee, prefiltered by a 100-μm mesh to exclude mesozooplankton. Weekly samplings of zooplankton with a 35-μm-mesh net confirmed that this procedure kept mesozooplankton at very low levels (<0.4 individuals L^{-1}) throughout the experiments (Diehl et al. 2002). In both years, we initially fertilized the enclosures with 7 μg L^{-1} dissolved inorganic phosphorus to final concentrations of total phosphorous of 16 μg L^{-1} (1997) and 14 μg L^{-1} (1998), respectively.

We sampled the enclosures weekly for a number of physical, chemical, and biological parameters. We measured photosynthetically active radiation (PAR) with a spherical quantum sensor (LI 193SA, LICOR) in each enclosure in steps of 1 m, beginning at the surface. PAR was also measured at 1.5 m in the shallowest enclosures in 1998. Water from each enclosure was collected in PE bottles and subsequently analyzed for dissolved nitrate and total phosphorus in both years and, in 1998, also for SRP and dissolved silica using standard methods. We took samples for phytoplankton counts with 200-ml glass bottles and immediately preserved them with Lugol's solution. To estimate sedimentation loss rates of phytoplankton, we suspended sedimentation traps just above the bottom of each enclosure. Each trap was a screw-lock glass jar (depth, 90 mm; opening diameter, 34 mm) with its lock removed. We retrieved and replaced traps at weekly intervals and preserved them with Lugol's solution. In 1997, no sedimentation traps were exposed during the first week. A more detailed description of the methods can be found in Diehl et al. (2002).

Enumeration and determination of the plankton samples—Phytoplankton in water samples and sedimentation traps was identified and counted in an inverted microscope (Utermöhl 1958). Thirty- to 50-ml subsamples were transferred to sedimentation chambers. After 16 h of sedimentation, we scanned an appropriately sized area to count at least 100 individual cells from each of the abundant taxa. For smaller taxa, we scanned at least two perpendicular transects across the sedimentation chamber. For larger taxa, such as dinoflagellates, ciliates, and rotifers, usually 50–100% of the chamber were scanned. In addition to light microscopy, some Lugol samples were cleaned according to Van der Werff (1955) and identified on a raster electron microscope. We identified all abundant phytoplankton taxa to species level except for the genera *Cyclotella* (*Bacillariophyceae*) and *Dinobryon* (*Chrysophyceae*). *Cyclotella* belonged mainly to the species *C. comensis* and *C. distinguenda* var. *mesoleia, Dinobryon* to *D. bavaricum, D. cylindricum, D. divergens*, and *D. sociale var. americanum*/*var. stipitatum* (Holzmann 1994; unpublished data of the authors).

Diatoms were identified according to Krammer and Lange-Bertalot (1986–1991), other taxa according to Popovsky and Pfiester (1990), Starmach (1985) and Tikkanen and Willén (1992). In both years, we measured individual cells, colonies, and filaments of the different taxa across a variety of samples. In each of those samples, about 30 individual cells, colonies, or filaments were measured per taxon. Within each experiment, these measurements did not indicate any systematic among-sample variation in the size distribution of the different taxa. We therefore used average dimensions (separately calculated for the 1997 and 1998 experiments) to calculate taxon-specific average biovolumes based on approximations of cell shapes by simple geometrical bodies given in Tikkanen and Willén (1992). For conversion to fresh algal biomass, a specific mass of 1 g ml^{-1} biovolume was assumed. Additionally, we measured dimensions of each common microzooplankton group (three different ciliates and two rotifers) and calculated their biovolumes by the same method.

Production and losses—To quantify production and losses of different phytoplankton taxa at different mixing depths, we calculated their net and gross growth rates as well as their sedimentation loss rates and sinking velocities over weekly intervals for each enclosure. Specific net production rate (p_n) was calculated as

$$p_n = \frac{1}{t}\ln\left(\frac{N_t}{N_0}\right) \quad (1)$$

where N_0 and N_t are the algal numbers per unit volume at time 0 and t, respectively. Specific sedimentation loss rate (l) was calculated as

$$l = p_n\left(\frac{C}{N_t - N_0}\right) \quad (2)$$

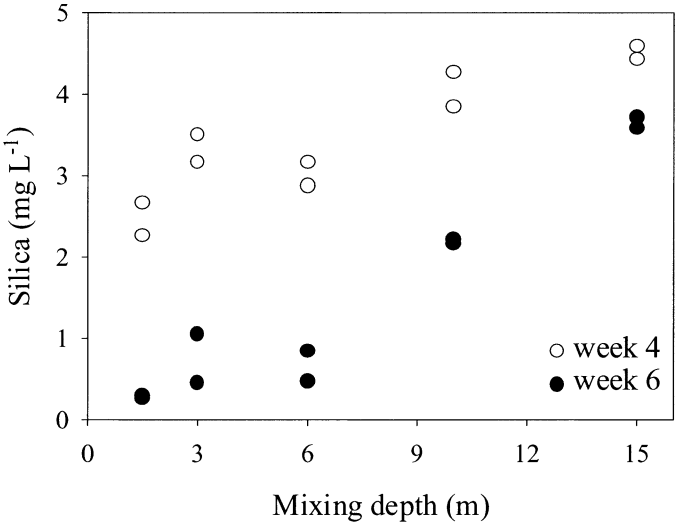

Fig. 2. Concentrations of soluble silica (mg L^{-1}) at the end of weeks 4 and 6 in the 1998 experiment.

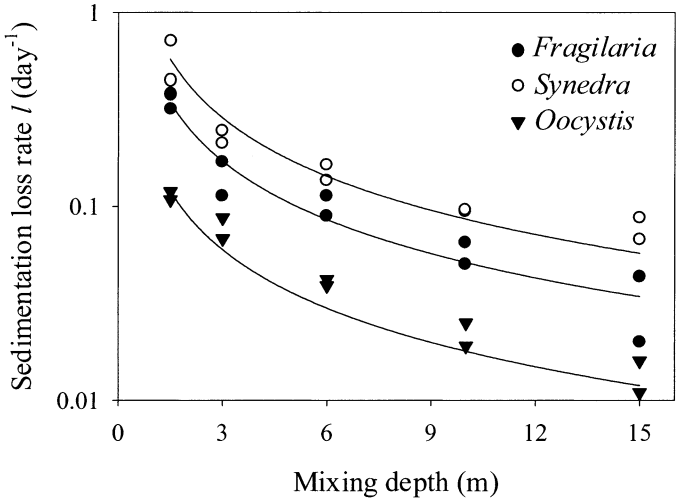

Fig. 3. Specific sinking loss rates of three sinking species in 1998, averaged over the experimental period for each enclosure. Solid lines show regression fits of Eq. 3. The resulting estimates of sinking velocity are given in Table 2.

where C is the number of algae per unit volume lost through sedimentation within time interval 0–t. For each enclosure, taxon-specific sedimentation loss rates were first calculated separately for each sampling date and then averaged over all available dates within an experiment (weeks 2–4 in 1997, weeks 1–6 in 1998). Average taxon-specific sedimentation loss rates were then plotted and regressed against mixing depth (z_{mix}; Fig. 3). Power functions with exponents close to -1 gave an excellent fit to the data. In order to obtain an estimate of taxon-specific sinking velocity (v'), we therefore fit the data to the theoretically expected form (Eq. 3; Reynolds 1984),

$$l = \frac{v'}{z_{mix}} \tag{3}$$

Refined estimates of the sedimentation loss rates l at different mixing depths were then obtained by plugging our estimate of v' back into Eq. 3. These refined estimates were then used to calculate taxon-specific gross growth (=production) rates (p) for each enclosure as

$$p = p_n + l \tag{4}$$

Light—Light intensity in the water column decreases approximately according to Lambert-Beer's law:

$$I_z = I_0 e^{-kz} \tag{5}$$

where I_0 is light intensity just below the surface, I_z is light intensity at depth z, and k is the specific light attenuation coefficient, representing the sum of abiotic background attenuation and biomass-dependent attenuation caused by phytoplankton. Using Eq. 5, we estimated k for each enclosure and each sampling date as the slope of a linear regression of log-transformed light intensity against depth. The average light intensity in the mixed water column (I_{mix}) was calculated as

$$I_{mix} = I_0\left(\frac{1 - e^{-kz_{mix}}}{kz_{mix}}\right) \tag{6}$$

Because our light measurements were too infrequent to be representative of average light conditions between samplings, we expressed average light intensity in relative terms as the percentage of incoming light by setting I_0 in Eq. 6 equal to 100.

Results

Light and nutrients—Results concerning phytoplankton resources (nutrients and light) are described in detail in Diehl et al. (2002) and only a very brief summary is given here. Average light intensity (I_{mix}, Eq. 6) decreased in both experiments with increasing mixing depth and was, at a given depth, about 50% lower in 1998 (high background turbidity) than in 1997 (moderate background turbidity). In 1998, concentrations of SRP and dissolved silica were positively related to mixing depth in the latter half of the experiment (SRP and silica were not measured in 1997). SRP was generally low (<2.5 μg L^{-1}) in all enclosures and decreased over time in the shallower enclosures (≤ 6 m), where it fell below the detection limit (1 μg L^{-1}) at the end of week 4 (Diehl et al. 2002). Contrary to SRP, concentrations of silica were rather high in all enclosures until the end of week 4 (Fig. 2). Thereafter, concentrations of silica declined markedly in the shallow enclosures and were 0.29 and 0.26 mg L^{-1} (1.5 m) at the end of week 6 (Fig. 2). Concentrations of nitrate always stayed above 3.5 mg L^{-1}. At all times, atomic ratios of dissolved nitrate and silicate to total phosphorus were above 800 (N) and 300 (Si), indicating that phosphorus was the growth-limiting nutrient in both experiments.

Microzooplankton—Abundances of ciliates and rotifers were investigated in order to assess their potential impact on phytoplankton net production. Most abundant within the microzooplankton were small- and medium-sized ciliates ($\simeq$20–50 μm equivalent spherical diameter). Additionally, rotifers were of significant abundance in some samples. Both

Table 1. Results from Spearman rank correlations between estimated biovolume of ciliates and rotifers, and the two smallest phytoplankton taxa. $n=50$ and 70 in 1997 and 1998, respectively. Correlation coefficients (coeff.) and P values.

		Ciliates		Rotifers	
	Year	Coeff.	P	Coeff.	P
Oocystis rhomboidea	1997	0.50	<0.001	0.34	0.015
	1998	−0.21	0.087	0.35	0.003
Rhodomonas minuta	1997	0.46	0.001	0.10	0.513
	1998	0.18	0.137	0.59	<0.001

groups graze on small phytoplankton (Sommer 1994). We therefore investigated their possible impact on the two smallest of the abundant taxa (*Oocystis rhomboidea* and *Rhodomonas minuta*; see section *Phytoplankton*) using Spearman rank correlation (Table 1). A negative correlation coefficient would indicate substantial grazing effects (top-down effect), whereas a positive correlation coefficient would suggest that microzooplankton benefited from feeding on the concerning phytoplankton taxon but did not influence its abundances substantially (bottom-up effect). In five out of eight cases, microzooplankton were positively correlated with the abundances of *Oocystis* or *Rhodomonas*; in two cases, no relationship was found; and only in one case, (*Oocystis* and ciliates in 1998) a nonsignificant, negative relationship was detected ($p = 0.09$; Table 1).

Phytoplankton—We report results from the eight most abundant phytoplankton taxa that could be identified unequivocally. Those taxa were the diatoms *Cyclotella* spec., *Fragilaria crotonensis, Synedra acus,* and *Asterionella formosa*; the chlorophyte *Oocystis rhomboidea*; the cryptophyte *Rhodomonas minuta*; the chrysophyte *Dinobryon* spec., and the dinoflagellate *Peridinium umbonatum. Asterionella* was only common in 1997, whereas *Peridinium* was only common in 1998. The remaining taxa were common in both years. Together, these eight taxa accounted for 80% (1997) and 76% (1998) of the overall phytoplankton biovolume (averaged over all depths and sampling dates). For these eight taxa, we first analyze how specific production and sedimentation loss rates depended on mixing depth, sinking velocity, light, and nutrient availability, and then describe how their biomass densities were affected by mixing depth, sinking velocity, and background turbidity.

Specific sedimentation losses—An important assumption of the model is that specific sedimentation loss rate is a decreasing function of mixing depth and an increasing function of sinking velocity (Eq. 3). *Rhodomonas, Dinobryon,* and *Peridinium* are flagellated, mobile taxa that should not sink out of the water column. We did indeed never find intact cells of *Dinobryon* and *Peridinium* in the sedimentation traps. We found few intact cells of *Rhodomonas* at times when *Rhodomonas* was very abundant, probably reflecting its high abundances in the water column rather than sedimentation losses. Consequently, we set the sinking velocities of these taxa to zero (Table 2). Specific sedimentation loss rates of the remaining, sinking taxa decreased with increasing mixing depth. The relationships between taxon-specific sedimentation loss rates and mixing depth were well described by Eq. 3 (Table 2; see examples in Fig. 3). Similar taxa differed between years in both their average sizes and their sinking velocities (Table 2) and were treated as independent data points in a correlation matrix of average sinking velocity against cell volume. Taxon-specific sinking velocity generally increased with increasing cell volume (Fig. 4, Spearman rank correlation, one-tailed $p = 0.029$). The lowest sinking velocity (0.18 m d^{-1}) was estimated for the small chlorophyte *Oocystis rhomboidea* in 1998 (sedimentation of *Oocystis* was not measured in 1997). The highest sinking velocities were estimated for the large diatoms *Fragilaria crotonensis,* 0.95 and 0.51 m d^{-1}, and *Synedra acus,* 0.62 and 0.86 m d^{-1}, in 1997 and 1998, respectively (Table 2).

Specific production—A central assumption of the model is that specific production (p) is limited by light and a mineral nutrient. To test the validity of this assumption, we performed multiple regressions using taxon-specific gross growth rates as response variables and average light intensity in the water column (I_{mix}) and the concentrations of dissolved nutrients (SRP, silica) as independent variables (forward selection of the independent variables, $p_{entry} = 0.05$, $p_{removal} = 0.1$). We included ambient resource levels both as linear and quadratic terms to allow for the possibility of saturating,

Table 2. Estimated average cell volumes (μm^3) and calculated mean sinking velocities v' (m day^{-1}) of the most abundant taxa in 1997 and 1998. Standard errors (SE), P, and r^2 values of the regression ($n=10$).

	1997					1998				
	Cell volume	v'	SE	P	r^2	Cell volume	v'	SE	P	r^2
Asterionella formosa	640	0.86	0.125	<0.001	0.92	*				
Cyclotella sp.	570	0.58	0.062	<0.001	0.94	303	0.46	0.065	<0.001	0.77
Fragilaria crotonensis	436	0.95	0.180	<0.001	0.87	251	0.51	0.025	<0.001	0.97
Synedra acus	3,000	0.62	0.088	<0.001	0.93	1,382	0.86	0.076	<0.001	0.90
Oocystis rhomboidea	150	†				42	0.18	0.011	<0.001	0.96
Rhodomonas minuta	170	0				54	0			
Dinobryon sp.	150	0				84	0			
Peridinium umbonatum	*					2,569	0			

* Not observed in this experiment.
† No sinking velocity estimated.

nonlinear relationships (Table 3). Silica was only included in the regression analysis for diatoms. Taxon-specific gross growth rates were separately calculated for each enclosure and over each (weekly) time interval between two sampling dates (see Materials and Methods). The corresponding nutrient and light availabilities were taken as the means of these two sampling dates. We performed multiple regressions only on the 1998 data because SRP and silica were not measured in 1997. Multiple regressions included data from all sampling dates during the entire (6-week) experimental period in 1998 (Table 3), but only from time intervals where a taxon was sufficiently abundant (at least 50 cells per sample).

The most striking pattern revealed by the multiple regressions (Table 3) is that specific gross growth rates of all four sinking taxa were strongly positively related to average light in the water column (I_{mix}). Relationships of *Synedra, Cyclotella,* and *Oocystis* with light were linear, whereas gross growth rates of *Fragilaria* were positively related to the linear and negatively related to the quadratic term of light. The maximum of this quadratic function falls in the range of the maximum observed light intensities, indicating light saturation at low mixing depths in *Fragilaria.* The gross growth rates of *Dinobryon* and *Peridinium* were not significantly related to light, though their abundances decreased monotonically with increasing mixing depth and therefore with decreasing light (Fig. 5). However, *Peridinium* was below the detection limit in the 10- and 15-m enclosures (Fig. 5), limiting the effective light gradient and weakening the power of the regression analysis. Gross growth rates of *Rhodomonas* were neither related to light nor to nutrient supply.

Specific gross production rates of three species (*Cyclotella, Dinobryon,* and *Peridinium*) were positively related to the concentrations of SRP. Because SRP reached the detection limit in the shallow enclosures in the second half of the experiment, the absence of a relationship between SRP and the gross production rates of the other taxa is possibly due to the low accuracy of the SRP measurements. The gross growth rates of the diatoms *Fragilaria* and *Synedra* were positively related to the quadratic and to the linear term of silica, respectively. The negative relationship of *Cyclotella* with the quadratic term of silica does not appear to be causal but may, in fact, indicate an opposite causal relationship (i.e., dissolved silica got depleted most strongly at shallow mixing depths where production of the diatoms was highest, Fig. 2).

Abundance patterns along the mixing depth gradient at low and high background turbidity—All other parameters being equal, the model predicts that the mixing depth, at which biomass density peaks (=depth of maximal abundance, DMA), should increase with increasing sinking velocity and decrease with increasing background turbidity (Fig. 1). To test these predictions, we first plotted the cell densities of the eight abundant taxa against mixing depth and estimated their DMAs (Fig. 5). We then performed an ANCOVA of the effects of background turbidity (fixed factor year) and taxon-specific sinking velocity (covariate) on the DMAs of the different taxa. With the exception of *Dinobryon,* we used data from the latest comparable sampling dates in both experiments (day 27 in 1997, day 28 in 1998).

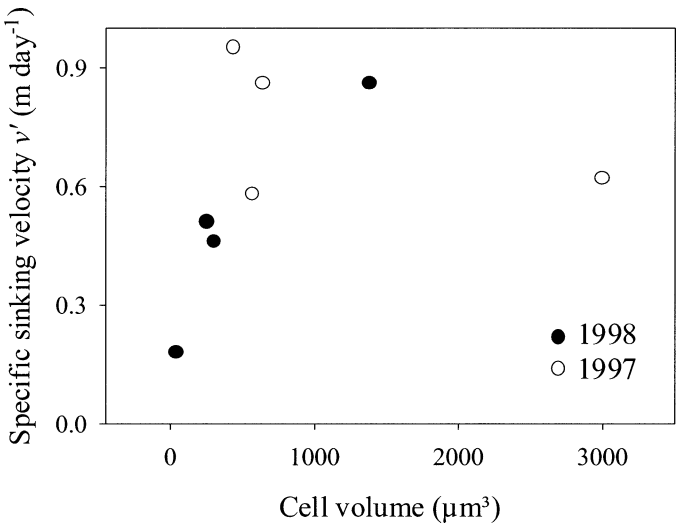

Fig. 4. Specific sinking velocity plotted against specific biovolume for the most abundant, sinking taxa in both experiments. Background turbidity was low in 1997 and high in 1998. The taxa are listed in Table 2.

We chose these dates because model predictions apply to a system at steady state and the phytoplankton communities underwent in both years only minor changes from week 3 to week 4. Abundances of *Dinobryon,* however, approached the detection limit on day 28 in 1998 in some enclosures. We therefore used data from the preceding sampling date (day 21), when *Dinobryon* was considerably more abundant. The general pattern (a monotonic decrease in *Dinobryon* density with increasing mixing depth, Fig. 5) was, however, the same on both dates. For each taxon and year, DMA (indicated by arrows in Fig. 5) was estimated as follows. If visual inspection of the data indicated either a monotonic or a unimodal pattern and the two highest cell densities occurred in the two replicates of the same mixing depth, this depth was defined as DMA. Otherwise, linear and quadratic regressions of the log-transformed cell densities versus mixing depth were performed. DMA was then defined as the depth at which a (statistically significant) regression line had its maximum within the experimental range of mixing depths (Table 4). If both regressions were statistically significant ($p < 0.05$), we chose the quadratic model if it increased the fit substantially (arbitrarily defined as an increase in r^2 by ≥ 0.1 compared with the linear model). If neither a linear nor a quadratic model could be fit to the data, an estimate of DMA could not be obtained.

The sinking taxa (*Asterionella, Cyclotella, Fragilaria, Synedra,* and *Oocystis*) showed in seven out of nine cases a unimodal pattern along the gradient of mixing depths (Fig. 5, Table 4). In addition, *Cyclotella* showed a monotonic increase with increasing mixing depth in 1997 (moderate background turbidity), whereas *Oocystis* decreased monotonically with increasing mixing depth in 1998 (high background turbidity). The motile species showed either a unimodal pattern (*Rhodomonas*) or a monotonic decrease (*Peridinium* and *Dinobryon* in 1998). No DMA could be determined for *Dinobryon* in 1997.

Table 3. Regression parameters of multiple linear regressions with weekly gross growth rates of the different taxa as response variables and average light intensity (I_{mix}), the concentrations of soluble reactive phosphorus (SRP), and soluble silica as independent variables. All independent variables were offered as linear (lin) and quadratic (quad) terms. Silica was included in the regression analysis only for diatoms. For each significant regression model, its r^2, P, and sample size n as well as the standard coefficients (Stand. coeff.) of the included independent variables, and their P are given.

	Regression			I_{mix}			SRP			Silica		
	r^2	P	n	Term	Stand. coeff.	P	Term	Stand. coeff.	P	Term	Stand. coeff.	P
Cyclotella	0.44	<0.001	55	lin	0.48	<0.001	lin	0.30	0.03	quad	−0.47	<0.001
Fragilaria	0.82	<0.001	35	lin	2.32	<0.001				quad	0.73	<0.001
				quad	−1.61	0.003						
Synedra	0.68	<0.001	34	lin	0.89	<0.001				lin	0.47	<0.001
Oocystis	0.21	<0.001	60	lin	0.46	<0.001					Not included	
Peridinium	0.34	0.001	29				lin	0.59	0.001		Not included	
Dinobryon	0.12	0.015	48				lin	0.35	0.015		Not included	
Rhodomonas	—	—	59								Not included	

As expected, DMA was negatively related to background turbidity (Fig. 6, ANCOVA, $p = 0.032$, $r^2 = 0.99$; year effect: $p = 0.015$). Also as expected, DMA was positively related to sinking velocity (Fig. 6) but, mainly because of one outlying data point (*Fragilaria* in 1997), this effect was only marginally significant in the ANCOVA ($p = 0.08$). When analyzed separately by year, DMA showed a significant positive relationship with sinking velocity in 1998 (linear regression, $p = 0.01$, $r^2 = 0.77$), but not in 1997 ($p = 0.47$, $r^2 = 0.14$).

Discussion

Patterns of sinking and nonsinking taxa along the mixing depth gradient (predictions 1 and 2)—The results confirm that trends seen for total biomass concentration (Diehl et al. 2002) were expressed by most nonmotile taxa, i.e., their abundances were generally limited by sedimentation losses at the shallow end and by low light at the deep end of the mixing depth gradient, leading to unimodal relationships between mixing depth and population density. This pattern deviates clearly from the pattern seen for productivity of these taxa that increased monotonically with increasing light as shown by the multiple regression analysis.

Also in agreement with expectations, two motile taxa declined monotonically with mixing depth. Only the cryptophyte *Rhodomonas minuta* deviated from expectations in both experiments, showing a unimodal trend similar to most sinking taxa. Because sedimentation cannot be the reason for this pattern, nutrient limitation and/or light inhibition may have limited its production at low mixing depths. This conclusion is in agreement with general findings about the ecology of cryptophytes, which have low requirements for light, but high requirements for mineral nutrients. These flagellates are frequently found in the metalimnion of stratified lakes or perform diurnal vertical migrations between deep and shallow layers (Klaveness 1989; Graham and Wilcox 2000).

Effects of sinking velocity on abundances and DMA (prediction 3)—Everything else being equal, an increase in sinking velocity should lead to lower abundances at any mixing depth. We did not test this prediction because taxa differing in sinking velocity likely differed in other characteristics (e.g., their affinities for limiting nutrients and light) as well. Furthermore, initial abundances of the different taxa were not equal.

We did, however, expect a positive relationship between the depths of maximal abundance (DMA) and the sinking velocities of the different taxa. This expectation was fulfilled in 1998, but not in 1997, largely because of an unexpectedly low DMA of *Fragilaria* in 1997. Additionally, the data suggest that, in 1997, the mixing depth gradient was too shallow to provide an estimate of a maximum in the depth-abundance distribution of *Cyclotella.*

Effect of background turbidity on abundances and DMA (prediction 4)—Everything else being equal, an increase in background turbidity should lead to lower abundances at any mixing depth. Again, we did not test this prediction because the different turbidity treatments were performed in different years with somewhat differing initial conditions and weather patterns (see Diehl et al. 2002).

We did, however, expect that DMA at a given sinking velocity was negatively affected by background turbidity. In agreement with this expectation, all sinking taxa except one (*Fragilaria crotonensis*) had maxima in their depth-abundance distributions at higher mixing depths in 1997 (moderate background turbidity) than in 1998 (high background turbidity). This result underlines that, in 1998, for almost all taxa, light was a strongly limiting factor at high mixing depths.

Effects of mixing depth on community composition—Although the experimental gradients in mixing depth created order-of-magnitude differences in sedimentation loss rates, the phytoplankton communities were dominated by sinking taxa at all mixing depths. At the end of week 4, diatoms made up more than 86% (1997) and 53% (1998) of the biovolume of the presented taxa in each enclosure (compare with Fig. 5). Diatoms persisted even in the shallowest enclosures, where specific sedimentation loss rates were as high as 0.5 day^{-1} (*Fragilaria* in 1997 at 2 m, *Synedra* in 1998 at 1.5 m). Maximal specific growth rates for these spe-

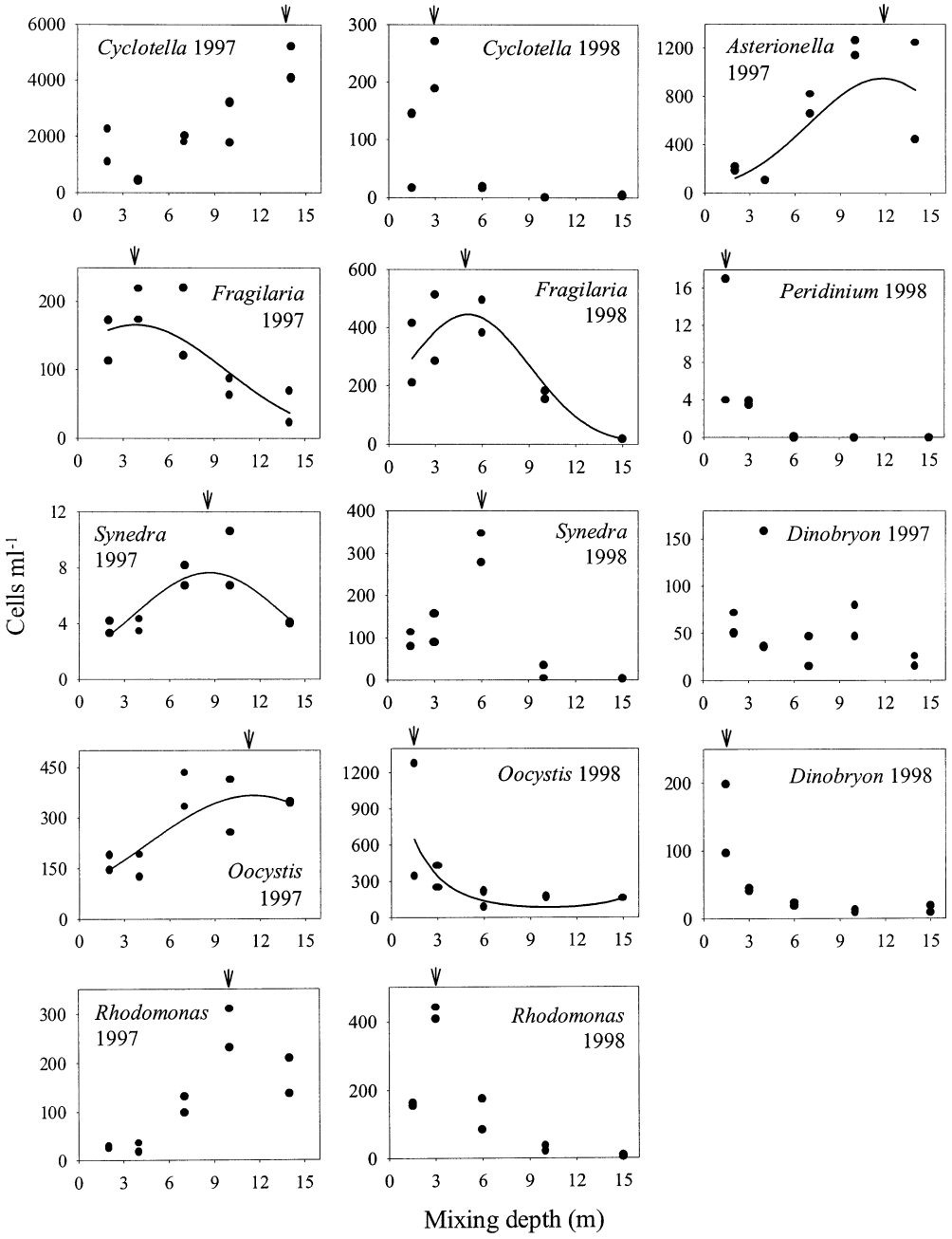

Fig. 5. Cell densities of the dominant taxa in relation to mixing depth at the end of week 4 in 1997 and 1998, respectively (data for *Dinobryon* in 1998 are from week 3). Depth of maximal abundance (DMA) is indicated by an arrow. If DMA was obtained by a regression, the corresponding regression line is shown.

cies (obtained from laboratory experiments) range from 0.5 to 1.0 and from 0.7 to 1.3 day^{-1} for *Fragilaria* and *Synedra*, respectively (Müller 1972; Sommer 1983 in Andersen 1997), suggesting that diatoms may have been able to outgrow competitors in spite of high loss rates. Diatoms are excellent competitors for dissolved phosphorus if silica is available in excess, as was the case in our systems (Kilham 1986; Grover 1997). Our results at shallow mixing depths seem to contrast somewhat with those of Reynolds et al. (1983, 1984), who observed in two enclosure experiments that diatoms were replaced by buoyant and flagellated taxa when mixing depth fell below 2 m. Reynolds et al. concluded that diatoms cannot persist in such shallow epilimnia due to high sedimentation losses. Contrary to our systems, their enclosures were, however, not artificially mixed and, thus, rather stagnant. Turbulent diffusion counteracts the directed movement of sinking algal cells (Reynolds 1984; Huisman et al. 2002) and it is therefore likely that the diatoms in our experiment suffered lower loss rates compared with those is the Reynolds et al. experiments.

Table 4. Depth of maximal abundance (DMA) of the eight most abundant taxa in week 4 of 1997 and 1998. If DMA was obtained as the maximum of a linear or quadratic regression (Quad reg), the corresponding P and r^2 values are given ($n=10$).*†

	1997				1998			
	DMA (m)	Method*	P	r^2	DMA (m)	Method	P	r^2
Asterionella formosa	11.78	Quad reg	0.022	0.66	Not observed			
Cyclotella sp.	14	By eye			3	By eye		
Fragilaria crotonensis	3.81	Quad reg	0.011	0.73	5.08	Quad reg	0.001	0.97
Synedra acus	8.62	Quad reg	0.012	0.72		By eye		
Oocystis rhomboidea	11.53	Quad reg	0.024	0.65	1.5	Quad reg	0.034	0.62
Rhodomonas minuta	10	By eye			3	By eye		
Dinobryon sp.	†				1.5	By eye		
Peridinium umbonatum	Not observed				1.5	By eye		

* Methods for determination of DMA: by eye (see text), or linear or quadratic regression.
† No DNA could be obtained.

Light levels at the bottom of the shallow enclosures were sufficient to sustain growth of sedimented diatoms. Thus, diatoms from the sediment may have constantly reinoculated the mixed water column. The proportion of diatoms in the water column was, however, very high throughout the entire experiment and we did not observe the build-up of a conspicuous benthic diatom population. Hence, although reinoculation from the sediment could explain persistence of diatoms in the shallowest enclosures, their observed dominance required sufficiently high growth rates in the plankton to counter sinking losses. It is worthwhile mentioning in this context that a high sinking velocity is not only to the disadvantage of an algal cell. Passive or active movement shortens contact time with the surrounding medium and facilitates nutrient uptake under limiting conditions (Berg and Purcell 1977; Smol et al. 1984; Pahlow et al. 1997). Fast sinking diatoms may therefore benefit from shorter contact times compared with more buoyant algae and from saving energy compared with (actively moving) flagellates.

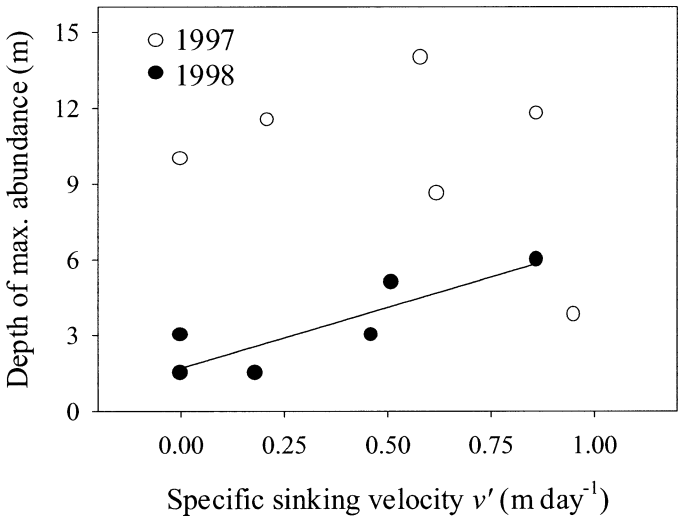

Fig. 6. Depth of maximal abundance (DMA) of the dominant species plotted against specific sinking velocity. Also shown is the significant regression line for the 1998 data (see text). Background turbidity was low in 1997 and high in 1998.

The contribution of *Fragilaria* and *Synedra* to overall phytoplankton biovolume was much higher in 1998 than in 1997 (compare abundances of *Fragilaria, Synedra,* and *Cyclotella* in 1997 with 1998, Fig. 5). It is possible that *Fragilaria* and *Synedra* benefited from high background turbidity in 1998, but a proper assessment of this hypothesis would require the manipulation of background turbidity in the same experiment.

Sinking losses and nutrient dynamics—Mixing depth in natural systems may vary from a few meters to some 10s of meters in lakes to more than 100 m in oceans. Thus, our enclosures covered only part of the range of natural mixing depths. This range seemed most interesting regarding the performance of diatoms in shallow mixed layers, and we have shown that diatoms can persist at very shallow depths if turbulence and the availability of silica are sufficiently high.

In our enclosures, sedimented algae were in touch with the mixed water column, allowing the recycling of mineralized nutrients. Our results are therefore most immediately applicable to situations in which the mixed layer is in direct contact with sediments (such as in shallow lakes or in deeper lakes during periods of destratification). At the shallowest mixing depths, the cumulative amount of particulate phosphorus that sedimented out of the water column over time exceeded the total phosphorus content of the water column at the beginning of the experiment (Diehl et al. 2002). This can only be explained by high mineralization rates of sedimented particulate phosphorus. In a system where the mixed surface layer is separated from the sediment by a stratified water column, return transport of sedimented nutrients back into the mixed layer is low. Compared with our experiments, this should lead to a stronger depletion of total nutrients and, consequently, to lower phytoplankton abundances and, possibly, a different taxonomic composition of the phytoplankton. Theoretical investigations suggest indeed that the presence or absence of a stratified water column below the mixed surface layer may have major implications for nutrient and plankton dynamics in the mixed layer (Diehl 2002). Future studies of mixing depth effects on plankton dynamics should therefore clearly distinguish between those two situations (Huisman and Sommeijer 2002; Yoshiyama and Nakajima 2002).

References

ANDERSEN, T. 1997. Pelagic nutrient cycles: Herbivores as sources and sinks. Springer.

BERG, H. C., AND E. M. PURCELL. 1977. Physics of chemoreception. Biophys. J. **20:** 193–219.

CONDIE, S. A., AND M. BORMANS. 1997. The influence of density stratification on particle settling, dispersion and population growth. J. Theor. Biol. **187:** 65–75.

DIEHL, S. 2002. Phytoplankton, light and nutrients in a gradient of mixing depths: Theory. Ecology **83:** 386–398.

———, BERGER, R. PTACNIK, AND A. WILD. 2002. Phytoplankton, light and nutrients in a gradient of mixing depths: Field experiments. Ecology **83:** 399–411.

ELLIOTT, J. A., A. E. IRISH, AND C. S. REYNOLDS. 2002. Predicting the spatial dominance of phytoplankton in a light-limited and incompletely mixed eutrophic water column using the PROTECH model. Freshwat. Biol. **47:** 433–440.

GRAHAM, L. E., AND L. W. WILCOX. 2000. Algae. Prentice Hall.

GROVER, J. P. 1997. Resource competition. Chapman & Hall.

HOLZMANN, R. 1994. Struktur und Dynamik von Phytoplankton-Gesellschaften: Eine vergleichende Analyse von 11 Seen der Naturschutzgebiete Eggestätt-Hemhofer Seenplatte und Seeoner Seen. Verlag Shaker, Aachen, Germany. [In German.]

HUISMAN, J. 1999. Population dynamics of light-limited phytoplankton: Microcosm experiments. Ecology **80:** 202–210.

———, M. ARRAYÁS, U. EBERT, AND B. SOMMEIJER. 2002. How do sinking phytoplankton species manage to persist? Am. Nat. **159:** 245–254.

———, AND B. SOMMEIJER. 2002. Population dynamics of sinking phytoplankton in light-limited environments: Simulation techniques and critical parameters. J. Sea Res. **48:** 83–96.

———, P. VAN OOSTVEEN, AND F. J. WEISSING. 1999. Critical depth and critical turbulence: Two different mechanisms for the development of phytoplankton blooms. Limnol. Oceanogr. **44:** 1781–1787.

———, AND F. J. WEISSING. 1995. Competition for nutrients and light in a mixed water column: A theoretical analysis. Am. Nat. **146:** 536–564.

KILHAM, S. S. 1986. Dynamics of Lake Michigan natural phytoplankton communities in continuous cultures along a Si:P loading gradient. Can. J. Fish. Aquat. Sci. **43:** 351–360.

KLAVENESS, D. 1989. Biology and ecology of the *Cryptophyceae*: Status and challenges. Biol. Oceanogr. **6:** 257–270.

KRAMMER, K., AND H. LANGE-BERTALOT. (1986–1991). *Bacillariophyceae,* v. 2 (1–4). *In* H. Ettel et al. [eds.], Freshwater flora of middle Europe. Gustav Fischer Verlag. [In German]

LUCAS, L. V., J. E. CLOERN, J. R. KOSEFF, S. G. MONISMITH, AND J. K. THOMPSON. 1998. Does the Sverdrup critical depth model explain bloom dynamics in estuaries? J. Mar. Res. **56:** 375–415.

LUND, J. W. G. 1971. An artificial alteration of the seasonal cycle of the plankton diatom *Melosira italica* susp. *subarctica* in an English lake. J. Ecol. **59:** 521–533.

MÜLLER, V. H. 1972. Wachstum und Phosphatbedarf von *Nitzschia actinatroides* (Lem.) von Goor in statischer und homokontinuierlicher Kultur unter Phosphatlimitierung. Arch. Hydrobiol. Suppl. **38:** 399–484. [in German]

PAHLOW M., U. RIEBESELL, AND D. A. WOLF-GLADROW. 1997. Impact of cell shape and chain formation on nutrient acquisition by marine diatoms. Limnol. Oceanogr. **8:** 1660–1672.

PETERSEN, J. E., C. C. CHEN, AND W. M. KEMP. 1997. Scaling aquatic primary productivity: Experiments under nutrient- and light-limited conditions. Ecology **78:** 2326–2338.

POPOVSKY, J., AND L. A. PFIESTER. 1990. *Dinophyceae* (*Dinoflagellidae*). *In* H. Ettel et al. [eds.], Freshwater flora of middle Europe. Gustav Fischer Verlag. [In German]

REYNOLDS, C. S. 1984. The ecology of freshwater phytoplankton. Cambridge Univ. Press.

———. 1988. Functional morphology and the adaptive strategies of freshwater phytoplankton, p. 388–433. *In* C. D. Sandgren [ed.], Growth and reproductive strategies of freshwater phytoplankton. Cambridge Univ. Press.

———, S. W. WISEMAN, AND M. J. O. CLARKE. 1984. Growth- and loss-rate responses of phytoplankton to intermittent artificial mixing and their potential application to the control of planktonic algal biomass. J. Appl. Ecol. **21:** 11–39.

———, ———, B. M. GOFREY, AND C. BUTTERWICK. 1983. Some effects of artificial mixing on the dynamics of phytoplankton populations in large limnetic enclosures. J. Plankton Res. **5:** 203–234.

RILEY, G. H. 1942. The relationship of vertical turbulence and spring diatom flowering. J. Mar. Res. **5:** 67–87.

SMAYDA, T. J., AND B. J. BOLEYN. 1965. Experimental observations on the flotation of marine diatoms. I. *Thalassiosira* cf. *nana, Thalassiosira rotula* and *Nitzschia seriata.* Limnol. Oceanogr. **10:** 499–509.

SMETACEK, V., AND U. PASSOW. 1990. Spring bloom initiation and Sverdrup's critical-depth model. Limnol. Oceanogr. **35:** 228–234.

SMOL, J. P., S. R. BROWN, AND H. J. MCINTOSH. 1984. A hypothetical relationship between differential algal sedimentation and diatom succession. Proc. Int. Assoc. Theor. Appl. Limnol. **22:** 1357–1360.

SOMMER, U. 1983. Nutrient competition between phytoplankton species in multispecies chemostat experiments. Arch. Hydrobiol. **96:** 399–416.

———. 1994. Planktology. Springer. [In German]

———, Z. M. GLIWICZ, W. LAMPERT, AND A. DUNCAN. 1986. The PEG-model of seasonal succession of planktonic events in freshwater. Arch. Hydrobiol. **106:** 433–471.

SOTO, D. 2002. Oligotrophic patterns in southern Chilean lakes: The relevance of nutrients and mixing depth. Rev. Chil. Hist. Nat. **75:** 377–393.

STARMACH, K. 1985. *Chrysophyceae* and *Haptophyceae,* v. 1. *In* H. Ettel et al. [eds.], Freshwater flora of middle Europe. Gustav Fischer Verlag. [In German]

SVERDRUP, H. U. 1953. On conditions of vernal blooming of phytoplankton. J. Cons. Perm. Int. Explor. Mer **18:** 287–295.

TIKKANEN, T., AND T. WILLÉN. 1992. Växtplanktonflora (Phytoplankton Flora). Swedish Environmental Protection Agency, Solna, Sweden. [In Swedish]

UTERMÖHL, H. 1958. Zur Vervollkommnung der quantitativen Phytoplankton-methodik. Int. Ver. Theor. Ang. Limnol. Mitteilungen **9:** 1–38. [in German]

VAN DER WERFF, A. 1955. A new method of concentrating and cleaning diatoms and other organisms. Proc. Int. Assoc. Theor. Appl. Limnol. **12:** 276–277.

VISSER, P. M., L. MASSAUT, J. HUISMAN, AND L. R. MUR. 1996. Sedimentation losses of *Scenedesmus* in relation to mixing depth. Arch. Hydrobiol. **136:** 289–308.

WALSBY, A. E., C. S. REYNOLDS, R. L. OLIVER, AND J. KROMKAMP. 1989. The role of gas vacuoles and carbohydrate content in the buoyancy and vertical distribution of *Anabaena minutissima* in Lake Rotongaio, New Zealand. Adv. Limnol. **32:** 1–25.

YOSHIYAMA, K., AND H. NAKAJIMA. 2002. Catastrophic transition in vertical distributions of phytoplankton: Alternative equilibria in a water column. J. Theor. Biol. **216:** 397–408.

Received: 18 September 2002
Accepted: 26 February 2003
Amended: 1 May 2003